Application of plasma columns to radiofrequency antennas

Gerard G. Borg[a] and Jeffrey H. Harris
Plasma Research Laboratory, Research School of Physical Sciences, Australian National University, Canberra ACT 0200, Australia

David G. Miljak
Wills Plasma Physics Department, School of Physics, University of Sydney, Sydney, New South Wales, 2006, Australia

Noel M. Martin
Defence Science and Technology Organisation, P.O. Box 1500, Salisbury, South Australia, 5108, Australia

(Received 3 November 1998; accepted for publication 9 April 1999)

Plasma offers a promising alternative to metal for a wide variety of radiofrequency antenna applications. In this letter we report measurements of efficiencies up to 50% and radiation patterns for plasma column antenna elements. It is demonstrated that the current distribution along the antenna can be controlled by the plasma density. Plasma columns can be used instead of metal elements in communications antennas. © *1999 American Institute of Physics.* [S0003-6951(99)04622-7]

The proposal to use plasma as the conductor in a radiofrequency (rf) antenna is not new. Recently, there has been a resurgence of interest in plasma antennas stemming mainly from the possibility of producing structures of low radar cross section.[1] In previous experiments, plasma has been produced by electrodes at opposite ends of the plasma column such as in a mains-driven fluorescent tube. This technique complicates construction and may lead to a disturbance of the antenna radiating properties, and increase in radar cross section, and worse noise performance.

Moisan, Shivarova, and Trivelpiece[2] and Burykin, Levitskiy, and Martynenko[3] have proposed that a plasma could be driven from one end of the column by excitation of the plasma surface wave. The need for two electrodes is eliminated and the plasma column projects from the feed point. The length of the column depends on the power used to drive the surface wave. For a monopole of length 2430 mm and diameter 38 mm, we achieved adequate illumination with less than 200 W of rf power; half of which was radiated at 30 MHz. Base band noise was low enough to permit clear, long-range communications from 3 to 150 MHz. Pulsed operation has also been demonstrated at 10% duty cycle (100 μs, on, and 1 ms, off) which allowed similar density plasmas to be produced at one tenth the average power consumption. This feature obtains, due to the long ($\sim$5 ms) plasma density, decay time versus the relatively short electron heating time for plasma tubes at modest filling pressures. For reception, dual-frequency operation can be employed where the received signal carrier is at one frequency and the plasma drive is at a different frequency.

The axisymmetric surface wave propagates along cylindrical plasma columns for frequencies lower than about the plasma frequency. If we neglect the fact that the current entrained by this wave must also radiate electromagnetic waves, then we may determine the wave-vector β for the surface wave from the plasma surface wave dispersion relation for an infinitely long column.[2] For a uniform plasma density, the wave vector along the plasma column β can be determined from

$$\epsilon_r T_0 I_1(T_{pa}) K_0(T_{0a}) + T_p K_1(T_{0a}) I_0(T_{pa}) = 0,$$

where $T_p^2 = \beta^2 - \epsilon_r k_0^2$ and $T_0^2 = \beta^2 - k_0^2$, a is the plasma column radius, k_0 is the free-space wave vector$=\omega/c$, $\epsilon_r = 1 - \omega_{pe}^2/\omega(\omega + i\nu)$ is the plasma dielectric constant, and ν is the electron–neutral collision frequency. The quantity $\omega_{pe}^2 = n_e e^2/m_e \epsilon_0$ is the electron plasma frequency where n_e is the plasma density. The K's and I's are Bessel functions. Figure 1(a) shows a plot of the real and imaginary parts of β vs ω/ω_{pe} for 30 MHz, $a = 0.0125$ m, and $\nu = 1$ GHz (typical of a fluorescent tube). At high densities where ω/ω_{pe} is small, the real part of β approaches the free-space wave vector k_0 and the damping rate given by Im$\{\beta\}$ is low. Here, the surface wave-induced current along the column is very similar to that propagating on a metallic dipole antenna. At low densities, however, the surface wave is heavily damped and has a shorter wavelength than would the current on a wire.

Now let us assume that the plasma column is suspended vertically above earth so as to be deployed as an antenna. From knowledge of the wave vector of the current along the column one can determine the current distribution, and hence, that portion of the resistance seen at its base terminals which would be dissipated in radio emission, i.e., the antenna radiation resistance. For example, for 1/4-wave resonance where the current has $\beta = k_0$, this portion of the resistance would be $\sim$36 Ω. Figure 1(b) plots the antenna radiation resistance as a gray-scale plot against ω/ν on the vertical axis and ω/ω_{pe} on the horizontal axis. Since collision frequencies from 10^6 to 10^9 Hz and densities $< 10^{18}\,\mathrm{m}^{-3}$ (plasma frequencies $< \sim$ 10 GHz) are typical for modest power plasma columns, we may conclude that a wide range of plasma conditions leads to a significant antenna radiation.

[a]Electronic mail: gerard.borg@anu.edu.au

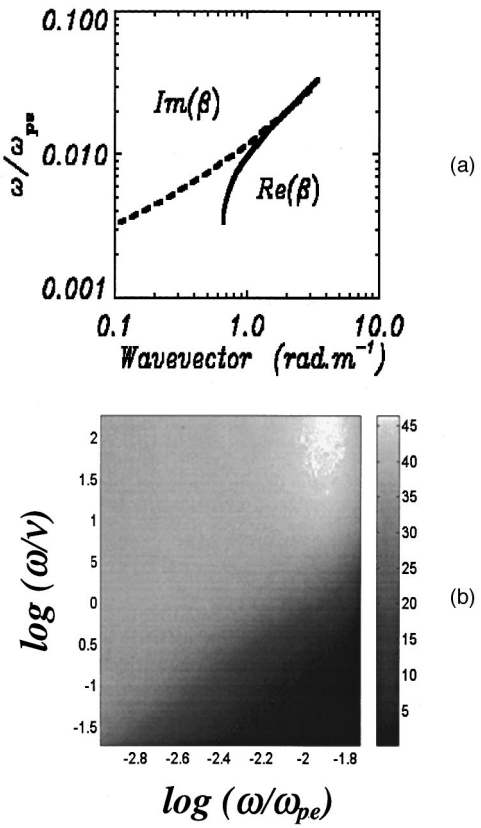

FIG. 1. (a) Solutions of the dispersion relation of the plasma surface wave at 30 MHz for a plasma tube of radius $a=0.0125$ m and $\nu=1$ GHz. (b) Contour plot of the antenna radiation resistance.

For low densities and high collisionality the antenna radiation resistance rapidly decreases.

Figure 2 shows a typical experimental arrangement. A copper cylindrical sleeve wrapped around the base of an electrodeless tube containing a low-pressure noble gas (typically, argon at ~1 Torr) couples an axisymmetric surface wave to the column. Usually, a fluorescent lamp was used for this purpose but without the usual mains circuitry. Unless otherwise stated, a matching network was employed to match the coupler to the rf generator.

Figure 3 shows experimental data for a 2430 mm plasma tube of 38 mm diam driven at 30 MHz. The wave is coupled capacitively by a sleeve of length 60 mm as shown in Fig. 2.

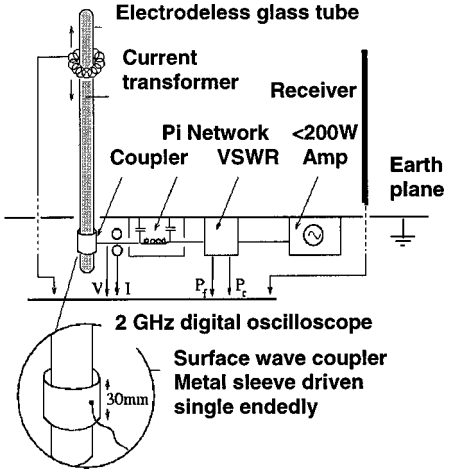

FIG. 2. Typical experimental arrangement.

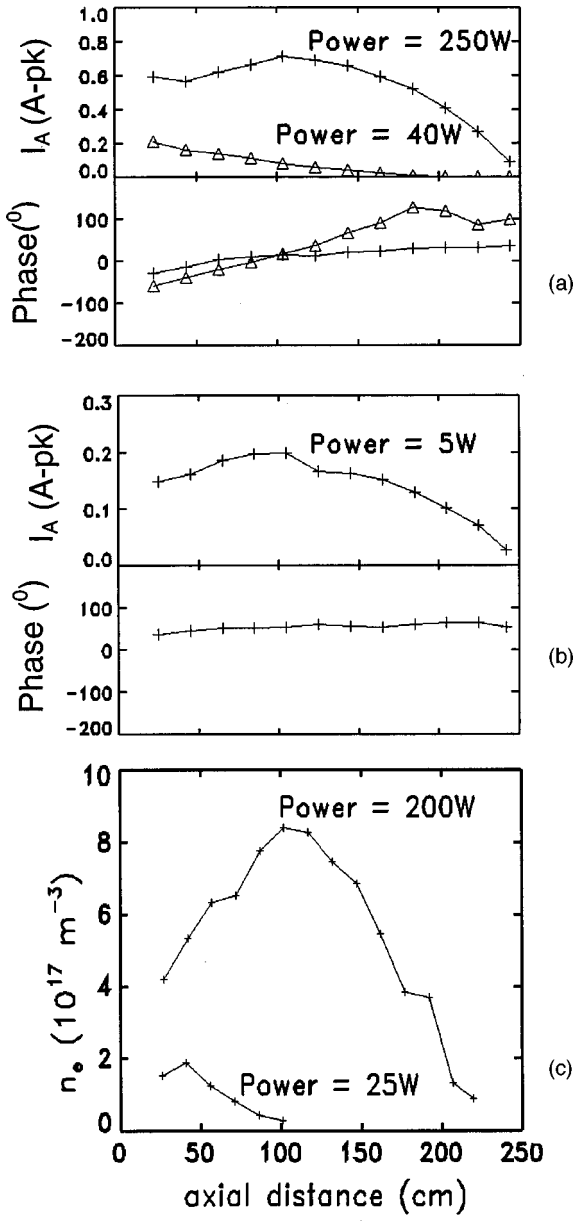

FIG. 3. (a) Amplitude (top) and phase (bottom) axial profiles along the tube at 35 MHz for high and low power. (b) Amplitude and phase axial profiles for the copper antenna. (c) Axial profiles of the line-integrated density for high and low power for a 2430 mm plasma tube driven at 30 MHz.

Measurements of the axial antenna current at 35 MHz (so that the antenna current was just beyond 1/4-wave resonance) are shown in Fig. 3(a). The top frame shows the current amplitudes for 250 and 40 W and the bottom frame the phases of the current along the column. The quoted powers are those into the matching network. Figure 3(b) shows the same measurements for a copper tube of the same length and diameter. The current distributions in Fig. 3(a) at 250 W and Fig. 3(b) are similar. The phases are also stationary in both cases as would be expected for a standing wave current. From the peak currents in each case, the efficiency of the plasma antenna is about 25% of the copper antenna. This result is not definitive because the actual currents and powers at the input to the coupling sleeve should be used in this calculation. Figure 3(c) shows the line-averaged density measured axially along a plasma column driven by the surface wave at 30 MHz for similar powers. At 200 W the

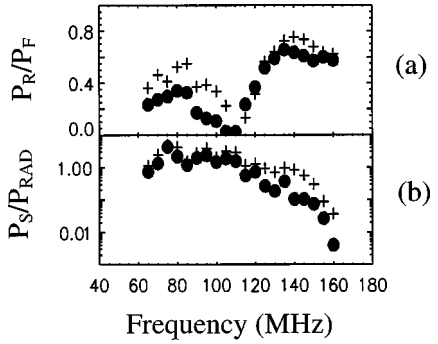

FIG. 4. Local radiation measurements as a function of frequency for a plasma antenna (filled circles) and copper antenna (''+'' symbols), each having identical geometry with length 614 mm and diameter 25 mm. (a) Ratio of reflected to forward power for each antenna. (b) Ratio of detected to transmitted powers for each antenna

plasma extends along the full length of the tube and is centrally peaked. The peak density of $4\times10^{17}\,m^{-3}$ corresponds to a plasma frequency of 5.7 GHz, much higher than the operating frequency. At 25 W, the plasma decays rapidly away from the sleeve in agreement with the exponential decay of the current in Fig. 3(a) at low power. In Fig. 3(a) at 40 W, the phase is an increasing function of distance along the tube corresponding to a phase speed of about 0.25 c. This behavior is in qualitative agreement with Fig. 1(a) and shows that the current distribution can be controlled by the plasma density.

The efficiency of an antenna is the ratio of radiated power to total power required to drive the antenna. The simplest way to measure it is to compare the amplitudes of the radiated fields for a given drive power into the plasma in the absence of matching network losses. The experimental setup is similar to Fig. 2. A copper and a plasma antenna each with length 614 mm and diameter 25 mm were compared. Plasma was formed by the signal to be transmitted without a matching network and was received 2000 mm away by a 129 MHz tuned receiving monopole. Figure 4(a) shows the ratio of reflected to forward power into the antenna. The plasma antenna results are represented by filled circles and the copper antenna by the ''+'' symbols. The results indicate that the tuning characteristics of the two antennas are similar. Figure 4(b) shows the normalized ratio of the received to transmitted signal power. The efficiencies are about 50% over the frequency range 60–120 MHz where the antennas are properly matched but taper significantly with increasing frequency as the coupling worsens and the plasma becomes more tenuous.

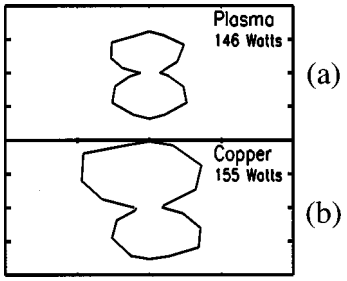

FIG. 5. Radiation patterns for (a) plasma and (b) copper half-wave dipoles.

Radiation patterns were recorded for a plasma and a copper half-wave dipole. The antennas were driven at 140 MHz and the received signal was recorded by a roaming 140 MHz, half-wave dipole. Figures 5(a) and 5(b) show the E-plane patterns for the plasma and copper antennas, respectively. The radial distance from the origin in Fig. 5 is proportional to the equatorial electric-field strength measured. As expected, these have the characteristic ''figure of 8.'' The scales are the same and indicate a 25% efficiency for the plasma antenna.

We conclude that efficiencies are high enough to make plasma antennas feasible for communications. Other properties of plasma antennas more relevant to reception and radar such as noise, will be presented in more expanded articles.

The authors gratefully acknowledge the technical support of Dennis Gibson, Con Costa, and Daniel Andruczyk, and useful discussions with Hunter Harris, D. Thorncraft, J. Howard, and R. W. Boswell. This work has been supported by the Australian Institute for Nuclear Science and Engineering and a contract between the Australian Defense Science and Technology Organization and the Research School of Physical Sciences and Engineering at the Australian National University.

[1] W. L. Kang, M. Rader, and I. Alexeff, 23rd IEEE International Conference on Plasma Science, Boston, MA, 3–5 June 1996, Paper No. 4IP07.
[2] M. Moisan, A. Shivarova, and A. W. Trivelpiece, Plasma Phys. **20**, 1331 (1982).
[3] Yu. I. Burykin, S. M. Levitskiy, and V. G. Martynenko, Radio Eng. Electron. Phys. **20**, 86 (1975).